Article

Serotonin and psilocybin activate 5-HT$_{1B}$ receptors to suppress cortical signaling through the claustrum

Maxwell B. Madden [ID][1], Chloe Schaefgen [ID][1], Binita Vedak[1,2], Jian Kwon [ID][1], Kiara S. Dresp Pedra[1], Samuel H. Sheats[1], Adam C. Puche[3,4], Steffen B. E. Wolff [ID][1,4] & Brian N. Mathur [ID][1,2,4,5] ✉

Through its widespread reciprocal connections with the cerebral cortex, the claustrum is implicated in sleep and waking cortical network states. Yet, basic knowledge of neuromodulation in this structure is lacking. The claustrum is richly innervated by serotonergic fibers, expresses serotonin receptors, and is suggested to play a role in the ability of psilocybin, which is metabolized to the non-specific serotonin receptor agonist psilocin, to disrupt cortex-wide network states. We therefore addressed the possible role of serotonin, and the classic psychedelic psilocybin, in modulating cortical signaling through the claustrum. We show that serotonin activates 5-HT$_{1B}$ receptors on anterior cingulate cortex inputs – a primary driver of claustrum activity – to suppress signaling to parietal association cortex-projecting claustrum neurons. Additionally, we demonstrate that psilocybin injection also activates anterior cingulate cortex presynaptic 5-HT$_{1B}$ receptors to suppress cortical signaling through the claustrum. Thus, serotonin, via 5-HT$_{1B}$, may provide gain-control of cortical input to the claustrum, a mechanism that may be directly targeted by psilocybin to modulate downstream cortical network states.

An organism's ability to successfully navigate complex environmental demands is determined by cognitive control of optimal behavioral responses. Cognitive control is shaped not only by external environmental demands, but by internal brain-states, both of which are supported through the activity of neuromodulator systems that project broadly across the brain[1-8]. Thus, the actions of neuromodulators on nuclei involved in cognition must be understood. Much work has investigated the contribution of the neuromodulatory monoamines, including serotonin (5-HT), dopamine, and norepinephrine, in cortical cognitive nodes, such as the prefrontal cortex (PFC)[8-15]. However, investigation in subcortical nuclei that may play critical roles in cortical networks subserving cognitive control is lacking.

The claustrum, a subcortical telencephalic nucleus, supports cortical networks[16-19] via cortico-claustro-cortical loops[20-22]. Receptors for 5-HT are enriched in the claustrum across multiple species[23-29] and the claustrum receives serotonergic input from the dorsal raphe nucleus[30]. The dorsal raphe nucleus is less active during sleep[31] and the claustrum produces synchronous cortical events during slow-wave sleep, but not during active wakefulness[32,33]. In humans, administration of psilocybin disrupts claustrum functional connectivity with several cortical networks and reduces the amplitude of low frequency fluctuations in claustrum BOLD signal[34]. Together, these data lead to speculation that the claustrum is targeted by 5-HT and related drugs[35-37] to modulate excitatory neurotransmission in cortico-claustro-cortical circuits.

[1]Department of Pharmacology and Physiology, School of Medicine, University of Maryland, Baltimore, MD, USA. [2]Department of Psychiatry, School of Medicine, University of Maryland, Baltimore, MD, USA. [3]Department of Neurobiology, School of Medicine, University of Maryland, Baltimore, MD, USA. [4]University of Maryland Medicine Institute for Neuroscience Discovery, University of Maryland, Baltimore, MD, USA. [5]Kahlert Institute for Addiction Medicine, University of Maryland, Baltimore, MD, USA. ✉e-mail: bmathur@som.umaryland.edu

Among the strongest cortico-claustro-cortical circuits is the connection between the ACC, through the claustrum, to the more posterior-lying parietal association cortex (PtA)[20]. Indeed, ACC input to the claustrum is dense[30,38,39] and is functionally significant: it is required for optimal performance in a cognitively demanding task[40]. Exploring the possibility that 5-HT may modulate signaling through this major pathway, we assayed the response of the ACC-claustrum synapse to 5-HT and found that 5-HT activated presynaptic 5-HT$_{1B}$ receptors to produce a synaptic depression. This effect was sufficient to depress signaling from ACC to PtA-projecting claustrum neurons. Additionally, we found that psilocybin injection also depressed claustrum signaling within the same population of neurons in a 5-HT$_{1B}$-dependent manner. These findings establish a synaptic mechanism for endogenous regulation of claustrum by 5-HT and suggest that the claustrum is directly targeted by psilocybin.

Results

5-HT-induced depression of the ACC-claustrum synapse

To determine effects of 5-HT on glutamatergic transmission from ACC to the claustrum, a channelrhodopsin2 (ChR2)-expressing virus was injected in ACC (Fig. 1A, B) and claustrum neurons (Fig. 1C) were targeted for recording of optically-evoked excitatory post-synaptic current (oEPSC) amplitudes before and after bath application of 5-HT (10 μM, 10 min) (Fig. 1D). Neurons received paired-pulse optical stimulation (50 ms inter-pulse interval) every 20 s, for 30 min, with bath application of 5-HT (10 μM, 10 min) occurring after a five-minute baseline. We observed that 5-HT application resulted in a depression of the first oEPSC event amplitude compared to baseline (two-tailed paired Student's t-test, $t_{10} = 3.43$, $p = 0.0064$, $n = 13$ neurons from 8 animals) or a no-drug control ($n = 6$ neurons, from 4 animals) (two-tailed Student's t-test, $t_{16} = 2.527$, $p = 0.0224$) (Fig. 1E–G). The observed depression was not accompanied by an increase in series resistance (Fig. 1E) and did not differ between males ($N = 6$, 1–3 neurons per animal) and females ($N = 9$, 1 neuron per animal) (two-tailed Student's t-test, $t_{13} = 0.24$, $p = 0.54$) (Figure S1).

In the same neurons, 5-HT (10 μM, 10 min) increased the paired pulse ratio (PPR) (EPSC2/EPSC1) compared to baseline (two-tailed paired Student's t-test, $t_{12} = 3.18$, $p = 0.007$) (Fig. 1F), suggesting a decrease in glutamate release probability. Correspondingly, the coefficient of variation (COV) of the first EPSC magnitude decreased compared to baseline (two-tailed paired Student's t-test, $t_{12} = 3.80$, $p = 0.002$). Application of 5-HT (10 μM, 10 min) in the presence of 500 nM tetrodotoxin (TTX) and 100 μM 4-Aminopyridine (4-AP) ($n = 10$ neurons, from 4 animals) elicited a synaptic depression (Fig. 1H) that was equal to that of the depression elicited from 5-HT (10 μM, 10 min) alone (two-tailed Student's t-test, $t_{14} = 0.017$, $p = 0.99$) (Fig. 1I–K). Thus, the 5-HT-mediated synaptic depression did not appear to be a polysynaptic effect.

5-HT$_{1B}$ receptor-mediated depression of ACC-claustrum synaptic transmission

As the change in PPR and COV indicated a presynaptic effect, we next tested if the 5-HT-mediated depression could be explained by 5-HT$_{1B}$, which is expressed presynaptically as a heteroreceptor[41–45] and is expressed in claustrum[28,46].

Continuing similar methodology (Fig. 2A), we found that application of a 5-HT$_{1B}$ receptor-selective agonist CP-93129 (10 μM, 10 min) induced depression of oEPSC amplitudes compared to baseline (two-tailed paired Student's t-test, $t_{10} = 4.81$, $p < 0.001$, $n = 11$ neurons, from 8 animals) and this depression was blocked by the presence of the specific 5-HT$_{1B}$ antagonist SB-216641 (20 μM, $n = 6$, from 4 animals) (two-tailed Student's t-test, $t_{15} = 2.90$, $p = .011$) (Fig. 2B–D). CP-93129 produced similar effects to 5-HT on PPR and COV, inducing an increase in PPR (two-tailed paired Student's t-test, $t_7 = 2.43$, $p = 0.046$, $n = 8$ neurons, from 8 animals) (Fig. 2C), and an increase in COV (two-tailed

paired Student's t-test, $t_8 = 3.80$, $p = 0.005$, $n = 8$ neurons, from 8 animals), suggesting a decrease in presynaptic transmitter release probability. The 5-HT$_{1B/D}$ antagonist, GR-127935 (20 μM) similarly blocked the CP-93129 (10 μM, 10 min) induced depression (two-tailed paired Student's t-test, $t_4 = 0.58$, $p = 0.59$, $n = 5$ neurons from 3 animals) (Fig. I). To determine if 5-HT$_{1B}$ may explain the entire 5-HT-mediated depression, we applied 5-HT (10 μM, 10 min, $n = 7$ neurons, from 7 animals) in the presence of SB-216641 (40 μM, $n = 6$ neurons, from 4 animals) (Fig. 2E). This significantly, but not fully, attenuated the 5-HT-mediated effect (two-tailed Student's t-test, $t_{10} = 2.83$, $p = 0.018$) (Fig. 2F–H).

Agonists and antagonists for 5-HT$_{1B}$ may have activity at 5-HT$_{1D}$. To ensure the specificity of our effects to 5-HT$_{1B}$ we applied CP-93129 (10 μM, 10 min) in the presence of a selective 5-HT$_{1D}$ antagonist, LY-310762 (10 μM) (Fig. 2J). LY-310762 failed to block the CP-93129 mediated depression of oEPSC amplitude responses (two-tailed paired Student's t-test, $t_4 = 5.89$, $p = 0.004$, $n = 5$ neurons from 4 animals). Additionally, we applied the selective 5-HT$_{1D}$ agonist, PNU-142633 (10 μM, 10 min) (Fig. 2K), which produced no change in the amplitude of oEPSC events (two-tailed paired Student's t-test, $t_5 = 0.33$, $p = 0.76$, $n = 6$ neurons from 3 animals) (Fig. 2K).

5-HT$_{1B}$ effects on spontaneous synaptic transmission

Thus far, the 5-HT$_{1B}$-mediated depression appeared to be presynaptically expressed. To confirm this, we applied 5-HT or CP-93129 and recorded excitatory spontaneous postsynaptic currents (sEPSCs) in the presence of 50 μM picrotoxin (PTX). Application of 5-HT (10 μM, 10 min) induced an increase in the interevent interval (IEI) of sEPSCs (two-tailed paired Student's t-test, $t_7 = 2.55$, $p = 0.038$, $n = 8$ neurons from 4 animals) with no change in sEPSC amplitude (two-tailed paired Student's t-test, $t_7 = 2.18$, $p = 0.066$, $n = 8$ neurons from 4 animals) (Fig. 3A), further supporting a decrease in presynaptic release probability. Application of the 5-HT$_{1B}$ agonist CP-93129 (10 μM, 10 min) increased sEPSC IEI (paired Student's t-test, $t_7 = 2.56$, $p = 0.037$, $n = 8$ neurons from 6 animals) with no change in the sEPSC amplitude (two-tailed paired Student's t-test, $t_7 = 0.21$, $p = 0.84$, $n = 8$ neurons from 6 animals) (Fig. 3B).

Spontaneous synaptic events arise from all inputs to claustrum neurons, not solely inputs from ACC. To assay ACC inputs specifically, we recorded claustrum neurons from animals that received injection of a ChR2-expressing virus to ACC, in an aCSF solution in which calcium was replaced with strontium (Fig. 3C–E). In the presence of strontium, vesicular release occurs asynchronously, allowing the analysis of vesicular release events from a specific input. Such asynchronous oEPSCs (a-oEPSCs) were identified in the 100 ms immediately after the first release event produced by optical stimulation, and the IEI and amplitude of a-oEPSCs were determined. Application of CP-93129 (10 μM, 10 min) produced no change in a-oEPSC amplitude (two-tailed paired Student's t-test, $t_{11} = 0.057$, $p = 0.96$, $n = 12$ neurons from 4 animals) but did produce a significant elevation in IEI (two-tailed paired Student's t-test, $t_{11} = 2.30$, $p = 0.042$, $n = 12$ neurons from 4 animals). Thus, sEPSC and a-oEPSC event analyses suggested that 5-HT$_{1B}$-mediated depression of the ACC-claustrum synapse occurred via a presynaptic mechanism.

Miniature excitatory postsynaptic currents (mEPSC) were subsequently recorded, via continuous presence of TTX (500 nM) and picrotoxin (50 μM) in the bath solution. 5-HT produced no change in either mEPSC IEI (two-tailed paired Student's t-test, $t_9 = 1.08$, $p = 0.31$, $n = 10$ neurons from 4 animals) or amplitude (two-tailed paired Student's t-test, $t_9 = 0.78$, $p = 0.46$, $n = 10$ neurons from 4 animals) of mEPSCs (Figure S2A), and CP-93129 similarly produced no change in IEI (two-tailed paired Student's t-test, $t_9 = 0.14$, $p = 0.89$, $n = 10$ neurons from 4 animals) or amplitude (two-tailed paired Student's t-test, $t_9 = 0.78$, $p = 0.46$, $n = 10$ neurons from 4 animals) (Fig. S2B). This suggested that the 5-HT- and CP-93129-mediated depression occurred
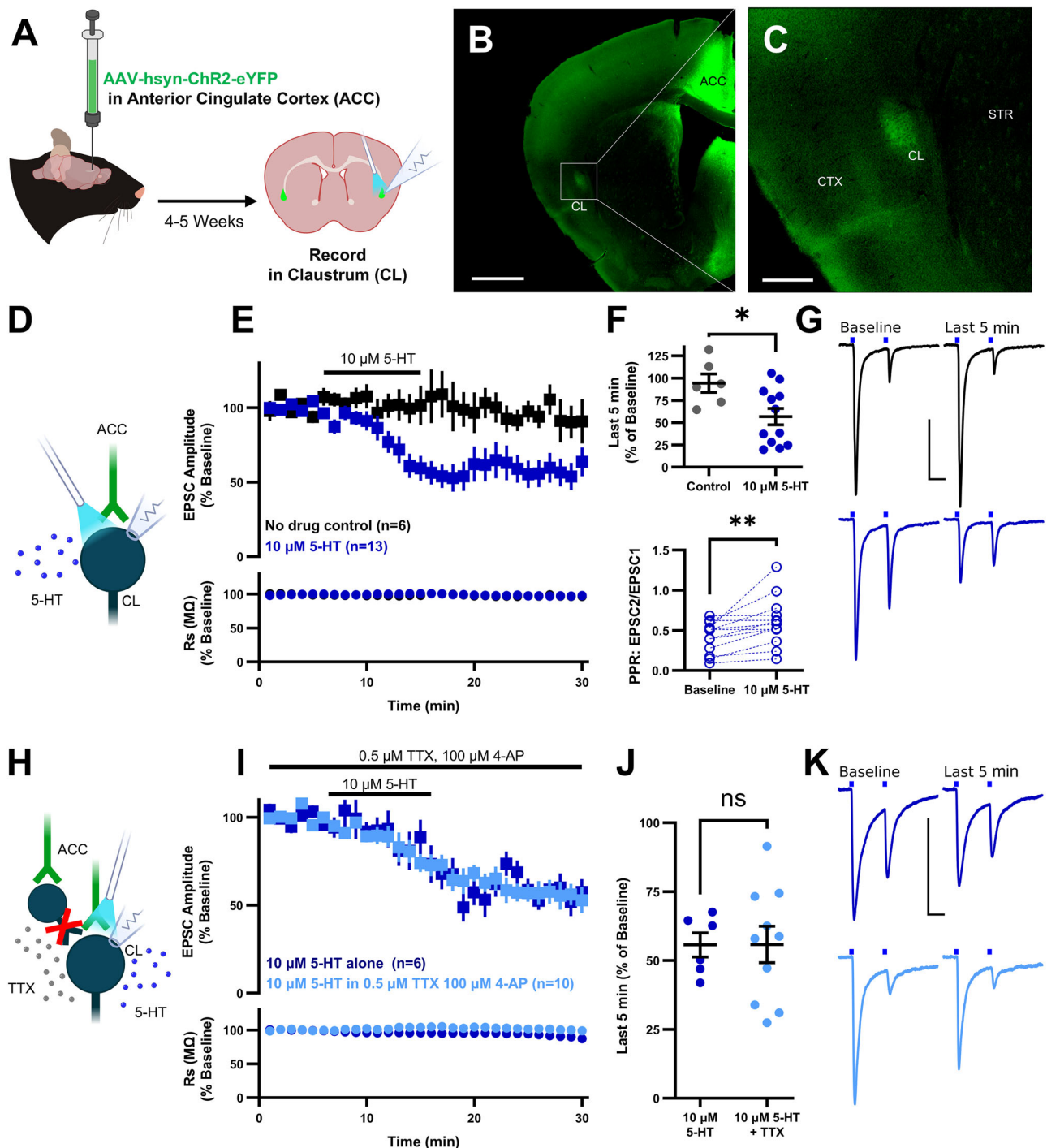
Fig. 1 | Serotonin (5-HT)-mediated presynaptic depression at the anterior cingulate cortex (ACC) to claustrum (CL) synapse. A Diagram detailing the experimental approach. **B** Representative image of the ACC injection site and terminal expression in claustrum. **C** Higher magnification of image in panel B depicting ACC terminal expression in the claustrum; Cortex (CTX) and striatum (STR) are also labeled. **D** Diagram of whole-cell patch recordings with optical stimulation of ACC terminals, corresponding to **E**–**G**. **E** 10 min of 10 µM 5-HT induced a depression of optically evoked post synaptic potential (oEPSC) amplitude. **F** Top, normalized oEPSC amplitude is significantly lower during the last five minutes of recording in neurons exposed to 10 min of 10 µM 5-HT (n = 13, from 8 animals) compared to a no-drug control (n = 6 neurons, from 4 animals) (two-tailed Student's t-test, $t_{16} = 2.53$, p = 0.022). Bottom, 5-HT (10 min, 10 µM) significantly increased paired-pulse ratio (PPR) (two-tailed paired Student's t-test, $t_{12} = 3.18$, p = 0.008, n = 13

neurons from 8 animals). **G** Representative traces of paired-pulse oEPSC events during baseline and the last five minutes of recording for both 5-HT-exposed neurons (blue) and no-drug control neurons (black). **H** Diagram of whole-cell patch recordings with optical stimulation of ACC terminals, corresponding to **I**–**K**. **I** The 5-HT- (10 min, 10 µM) mediated depression of oEPSC amplitude persisted in the presence of TTX and 4-AP. **J** The oEPSC amplitude during the last 5 min of recording is not significantly different between 5-HT/TTX/4-AP (n = 10, from 4 animals) or 5-HT alone (n = 6, from 4 animals) conditions (two-tailed Student's t-test, $t_{14} = 0.017$, p = 0.99). **K** Representative traces of paired-pulse oEPSC events during baseline and last five minutes of recording for both TTX/4-AP/5-HT (light blue) and 5-HT alone (dark blue) conditions. Scale bars are 1 mm for B, 0.3 mm for C, 25 ms (horizontal) by 200 pA (vertical) for G and K. All error bars represent standard error of the mean (SEM). Source data are provided as a Source Data file.
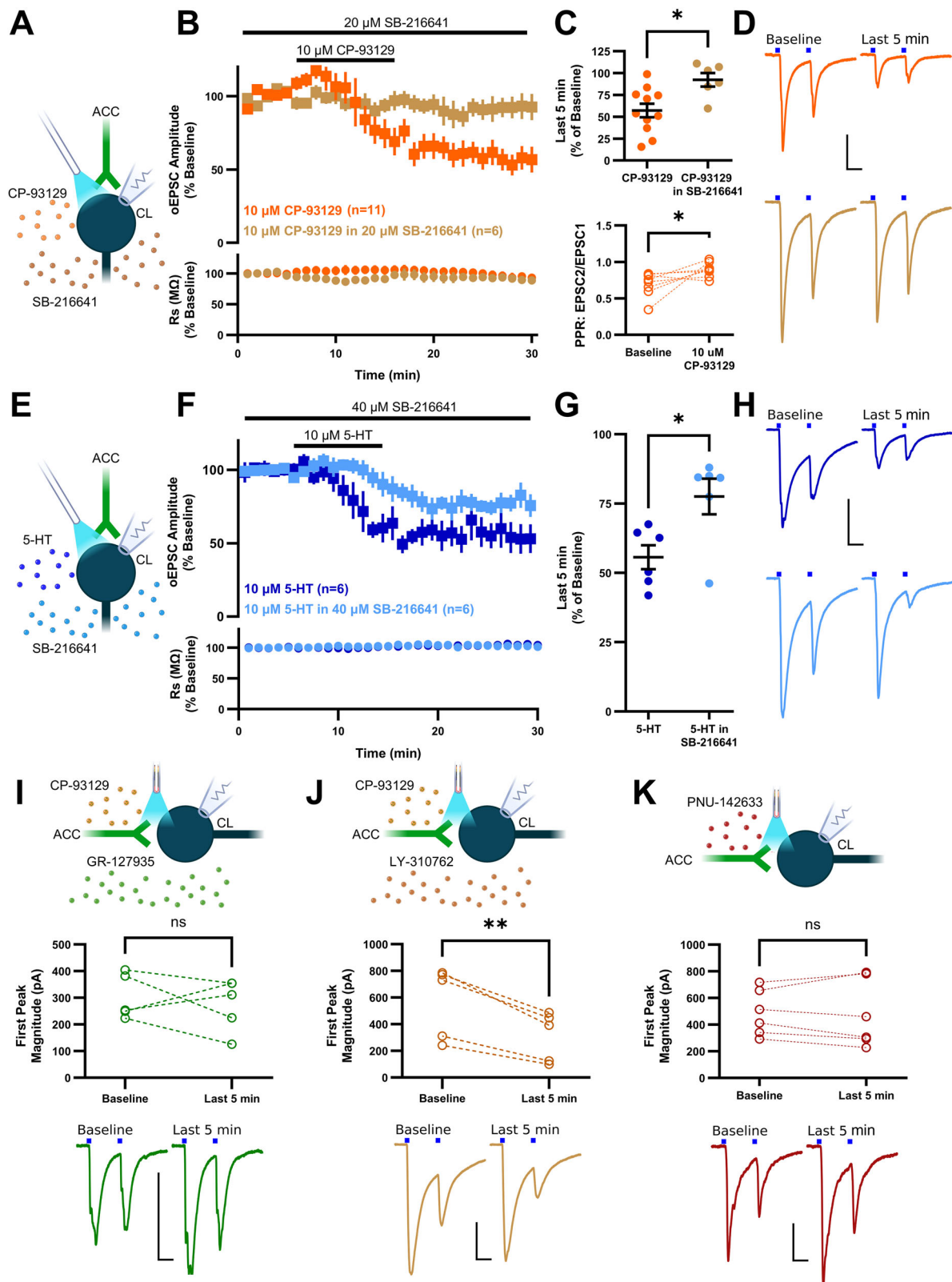
through alterations of the excitability of the presynaptic axon terminal rather than direct interaction with the protein machinery of vesicular release[47].

5-HT or 5-HT$_{1B}$ agonist suppression of ACC input to PtA-projecting claustrum neurons

Considering that we observed a depression of the ACC-claustrum synapse, we next sought to determine whether 5-HT- or a 5-HT$_{1B}$

agonist suppressed signaling onto projection-specified claustrum neurons. The PtA-projecting neurons were chosen as claustrum neurons that project to the PtA have the largest excitatory responses to ACC input compared to neurons that project to other cortical regions[20]. To do this, we injected AAV-hSyn-ChR2-EYFP into ACC and retrogradely transported rgAAV-CAG-tdTomato into PtA (Fig. 4A–D). Retrogradely-labeled tdTomato-positive claustrum neurons were then recorded while optically stimulating ACC inputs to produce optically

Fig. 2 | 5-HT-induced depression of the ACC-claustrum synapse: 5-HT$_{1B}$ dependence. A Diagram of whole-cell patch recordings with optogenetic stimulation of ACC terminals, corresponding to **B**–**D**. **B** CP-93129 (10 µM, 10 min), a specific 5-HT$_{1B}$ agonist, induced a depression of the ACC-claustrum synapse (two-tailed paired Student's t-test, t_{10} = 4.81, p <.001, n = 11 neurons from 8 animals) that was blocked by SB-216641 (20 µM, 10 min), a specific 5-HT$_{1B}$ antagonist. **C** Top, comparison of the magnitude of oEPSC amplitude during the last five minutes of recording after 10 µM CP-39129 exposure (n = 11, from 8 animals) or 20 µM SB-216641 (n = 6, from 4 animals) (two-tailed Student's t-test, t_{15} = 2.90, p = 0.01). Bottom, PPR significantly increased after exposure to 10 µM CP-93129 (two-tailed paired Student's t-test, t_7 = 2.43, p = 0.046, n = 8 neurons from 8 animals). **D** Representative oEPSC events during baseline and last five minutes of recording for both 10 µM CP-93129 exposed neurons (orange) and 10 µM CP-93129 in 20 µM SB-216641 exposed neurons (light brown). **E** Experimental diagram corresponding to **F**–**H**. **F** The 5-HT-induced depression of the ACC-claustrum synapse was blocked by 40 µM SB-216641. **G** Comparison of the magnitude of oEPSC amplitudes during the last five minutes of recording for 10 µM 5-HT exposed cells in normal aCSF (n = 7, from 7 animals) or 40 µM SB-216641 (n = 6, from 4 animals) (two-tailed Student's t-test, t_{10} = 2.83, p = 0.01). **H** Representative oEPSC events during baseline and the last five minutes of recording for both 10 µM 5-HT (blue) and 10 µM 5-HT in 40 µM SB-216641 (light blue) conditions. **I** Top, experimental diagram corresponding to this panel. Middle, CP-93129 (10 µM, 10 min) did not induce a change in oEPSC amplitude while in the presence of GR-127935 (20 µM), a 5-HT$_{1B/D}$ antagonist (two-tailed paired Student's t-test, t_4 = 0.58, p = 0.59, n = 5 neurons from 3 animals). Bottom, representative oEPSC events during baseline and after exposure to CP-93129 (10 µM, 10 min) in GR-127935 (20 µM) aCSF. **J** Top, experimental diagram corresponding to this panel. Middle, CP-93129 (10 µM, 10 min) depressed the ACC-claustrum synapse in the presence of LY-310762 (10 µM), a selective 5-HT1$_D$ antagonist (two-tailed paired Student's t-test, t_4 = 5.89, p = 0.004, n = 5 neurons from 4 animals). Bottom, representative oEPSC events during baseline and after exposure to CP-93129 (10 µM, 10 min) in LY-310762 (10 µM). **K** Top, experimental diagram corresponding to this panel. Middle, PNU-142633 (10 µM, 10 min), a specific 5-HT1$_D$ agonist, did not alter oEPSC amplitude (two-tailed paired Student's t-test, t_5 = 0.33, p = 0.76, n = 6 neurons from 3 animals). Bottom, representative oEPSC events during baseline after exposure to PNU-142633 (10 µM). Scale bars are 25 ms (horizontal) by 200 pA (vertical) for **D**, **H**, and **I**–**K** bottom. All error bars represent SEM. Source data are provided as a Source Data file.

evoked excitatory postsynaptic potentials (oEPSPs) or action potentials (APs) (Fig. 4F), thus specifically isolating input from ACC to PtA-projecting claustrum neurons. As extended recordings may incur changes in resting membrane voltage, we elected to record tdTomato-labeled neurons within the same claustrum slices before and after temporary application of 5-HT (10 µM, 10 min) to assess alterations in signaling. To capture the full dynamic range of potential responses, optical stimulation was performed across a range of stimulation intensities. For each light intensity, three stimulation events were delivered with an interpulse interval of 150 ms. This was repeated every 20 seconds over the course of one minute (for a total of nine stimulation events). This protocol was repeated across the following light intensities: 3.2 mW (100% intensity) 2.56 mW (80%), 1.92 mW (60%), 1.28 mW (40%), 0.64 mW (20%), and 0 mW (0%). The average number of APs per light pulse stimulation (APs/LP) and the area under the curve (AUC) of the voltage response were determined and averaged across all light intensities as measures of functional circuit strength, matching previous protocols[20].

Neurons recorded after temporary exposure to 5-HT (10 µM, 10 min, n = 12 neurons, from 5 animals) showed lower AUC (two-tailed Student's t-test, t_{22} = 2.10, p = 0.048) and APs/LP (two-tailed Student's t-test, t_{22} = 2.10, p = 0.048) compared to neurons from the same slices recorded prior to exposure (n = 12 neurons, from the same 5 animals) (Fig. 4G, H, S3A-B). In the same neurons, we observed no differences in measures of intrinsic excitability or cell properties between 5-HT (10 µM, 10 min) exposed and unexposed cells, including membrane capacitance (two-tailed Student's t-test, t_{22} = 1.78, p = 0.089), resting membrane potential (two-tailed Student's t-test, t_{22} = 0.96, p = 0.35), input resistance (two-tailed Student's t-test, t_{20} = 1.04, p = 0.31), membrane resistance (two-tailed Student's t-test, t_{22} = 0.33, p = 0.74), rheobase (two-tailed Student's t-test, t_{20} = 1.24, p = 0.23), or AP threshold (two-tailed Student's t-test, t_{20} = 0.94, p=0.36) (Figure S4 A-G).

Correspondingly, after temporary exposure to the 5-HT$_{1B}$ agonist CP-93129 (10 µM, 10 min, n = 15 neurons, from 4 animals) (Fig. 4I), neurons also showed lower AUC (two-tailed Student's t-test, t_{27} = 2.30, p = 0.030) and APs/LP (two-tailed Student's t-test, t_{29} = 2.36, p = 0.025) compared to unexposed neurons from the same slices recorded prior to exposure (n = 14 neurons) (Figs. 4J–K, 3C–D). Thus, the suppression of ACC signaling to PtA-projecting claustrum neurons by 5-HT may be mediated by 5-HT$_{1B}$. In the same neurons, following application and washout of CP-93129 (10 µM, 10 min) we also observed no changes in membrane capacitance (t_{27} = 1.89, p = 0.070, two-tailed Student's t-test), resting membrane potential (two-tailed Student's t-test, t_{26} = 0.22, p=0.83), input resistance (two-tailed Student's t-test,

t_{27} = 0.70, p = 0.49), membrane resistance (two-tailed Student's t-test, t_{26} = 0.75, p = 0.46), rheobase (two-tailed Student's t-test, t_{26} = 0.60, p = 0.55), or action potential threshold (two-tailed Student's t-test, t_{26} = 0.09, p = 0.93) (Fig. S4H–N).

Psilocybin induced, 5-HT$_{1B}$ receptor-mediated suppression of signaling from ACC to PtA-projecting claustrum neurons

The classic psychedelic drug psilocybin is metabolized to psilocin, which is a pan-serotonin receptor agonist[48]. To determine if psilocybin similarly suppressed signaling from ACC to PtA-projecting claustrum neurons, we first performed viral injections as before (AAV-hSyn-ChR2-EYFP into ACC and retrogradely transported rgAAV-CAG-tdTomato into PtA) and 5-6 weeks were allowed for expression. Mice were then injected 1 mg/kg psilocybin or equivalent volume of saline (i.p.) prior to recording head twitch events for 30 min. Head twitches are rapid head movements occurring in mice after psychedelic drug administration, which are mediated by 5-HT$_{2A}$[48-50]. Thus, the presence of head twitches was used to confirm the central efficacy of psilocybin. After the 30 min of head twitch recordings, mice were then euthanized, brains sliced and oEPSPs or APs recorded as described above (Fig. 5A). Head twitch events were elevated in the psilocybin injected animals (N = 10 animals) compared to vehicle controls (N = 10 animals) (two-tailed Student's t-test, t_{18} = 12.45, p < 0.0001) (Fig. 5B), confirming the efficacy of the drug. AUC and APs/LP for each neuron recorded were averaged for all neurons within a given animal (4-10 neurons per animal), and the average AUC and APs/LP for each animal were compared across groups. Psilocybin-injected animals had lower AUC (two-tailed Student's t-test, t_{18} = 2.67, p = 0.016) and APs/LP (t_{18} = 2.26, p = 0.036) (Figs. 5C, D, S5A-B) compared to vehicle-injected animals. Animals injected with psilocybin (1 mg/kg) showed no difference in membrane capacitance (two-tailed Student's t-test, t_{27} = 1.89, p = 0.070), resting membrane potential (two-tailed Student's t-test, t_{26} = 0.22, p = 0.83), input resistance (two-tailed Student's t-test, t_{27} = 0.70, p = 0.49), membrane resistance (two-tailed Student's t-test, t_{26} = 0.75, p = 0.46), rheobase (two-tailed Student's t-test, t_{26} = 0.60, p = 0.55), or action potential threshold (two-tailed Student's t-test, t_{26} = 0.09, p = 0.93) compared to vehicle controls (Fig. S4 O–U).

Next, to determine if the observed psilocybin-mediated suppression was 5-HT$_{1B}$- dependent, we pre-injected animals with the selective 5-HT$_{1B/D}$ antagonist GR-127935 (10 mg/kg, N = 12 animals) or saline (N = 12 animals) 15 min before injection with 1 mg/kg psilocybin, recording head twitch events before slicing and performing fluorescence-guided patch-clamp recordings as before (4-7 neurons per animal) (Fig. 5E). Head twitches were unaltered between the GR-127935 and saline pre-injected groups (two-tailed Student's t-test,
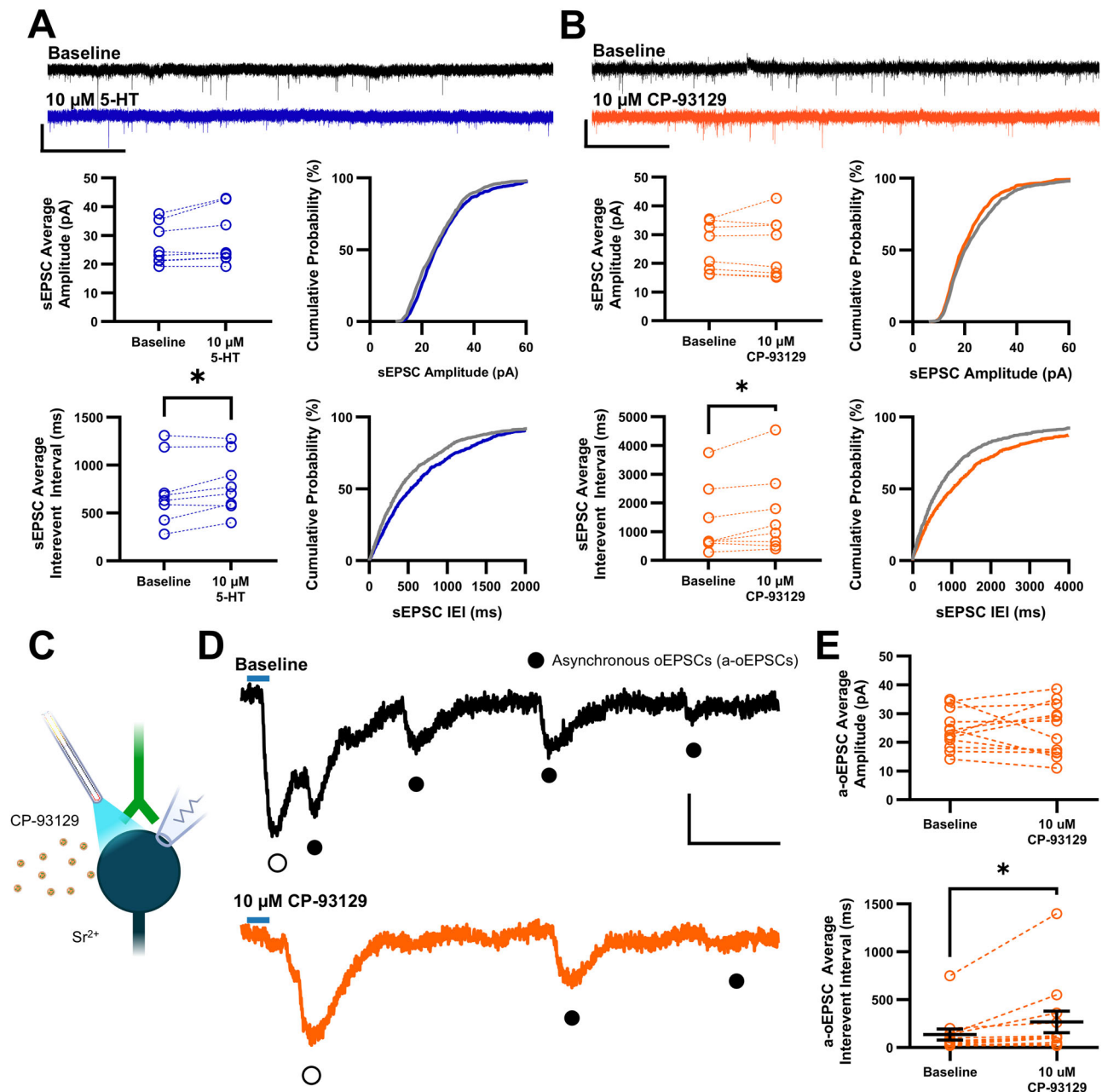
Fig. 3 | 5-HT or CP-93219 decreased the frequency of spontaneous EPSC (sEPSC) events. A Top, representative sEPSC events before and after exposure to 10 μM 5-HT for 10 min. Middle left, 10 μM 5-HT did not alter sEPSC amplitude (two-tailed paired Student's t-test, $t_7 = 2.18$, p = 0.066, n = 8 neurons from 4 animals). Middle right, cumulative probability plot of sEPSC amplitude before (gray) and after (blue) exposure to 10 μM 5-HT. Bottom left, exposure to 10 μM 5-HT increased the interevent interval (IEI) of sEPSCs (two-tailed paired Student's t-test, $t_7 = 2.55$, p = 0.038, n = 8 neurons from 4 animals). Bottom right, cumulative probability plot of sEPSC IEI before (gray) and after (blue) exposure to 10 μM 5-HT. **B** Top, representative sEPSC events before and after exposure to 10 μM CP-93129 for 10 min. Middle left, 10 μM CP-93129 did not alter sEPSC amplitude (two-tailed paired Student's t-test, $t_7 = 0.21$, p = 0.84, n = 8 neurons from 6 animals). Middle right, cumulative probability plot of sEPSC amplitude before (gray) and after (blue)

exposure to 10 μM CP-93129. Bottom left, 10 μM CP-93129 increased the interevent interval (IEI) of sEPSC events (two-tailed paired Student's t-test, $t_7 = 2.56$, p = 0.037, n = 8 neurons from 4 animals). Bottom right, cumulative probability plot of sEPSC IEI before (gray) and after (blue) exposure to 10 μM CP-93129. **C** Experimental diagram corresponding to **D** and **E**. **D** Representative a-oEPSCs elicited by stimulation of ACC terminals at baseline and after exposure to 10 μM CP-93129 for 10 min. **E** Top, 10 μM CP-93129 did not alter a-oEPSC amplitude (two-tailed paired Student's t-test, $t_{11} = 0.057$, p = 0.96, n = 12 neurons from 4 animals). Bottom, 10 μM CP-93129 increased interevent interval of a-oEPSCs elicited by ACC terminal activation (two-tailed paired Student's t-test, $t_{11} = 2.30$, p = 0.042, n = 12 neurons from 4 animals). Scale bars are 5 s (horizontal) by 20 pA (vertical) for **A** and **B**, top. Scale bars are 20 ms (horizontal) by 40 pA (vertical) for **D**. All error bars represent SEM. Source data are provided as a Source Data file.

$t_{22} = 0.91$, p = 0.37) (Fig. 5F), confirming that GR-127935 was not modulating psilocybin's action as a 5-HT$_{2A}$ agonist[48,50]. GR-127935 (10 mg/kg) pre-injected animals showed higher AUC (two-tailed Student's t-test, $t_{22} = 2.55$, p=0.018) and APs/LP (two-tailed Student's t-test, $t_{22} = 2.73$, p = 0.012) compared to animals that received saline pre-injection (Figs. 5G, H, S5C–D). This suggested that 5-HT$_{1B}$ is

required for psilocybin-induced depression of ACC synapses onto PtA-projecting claustrum neurons.

To examine if the psilocybin-mediated depression of ACC signaling to PtA-projecting claustrum neurons remained stable over time, we injected animals with either saline (N = 14 animals) or psilocybin (1 mg/kg, N = 13 animals), recorded head twitches, and allowed a
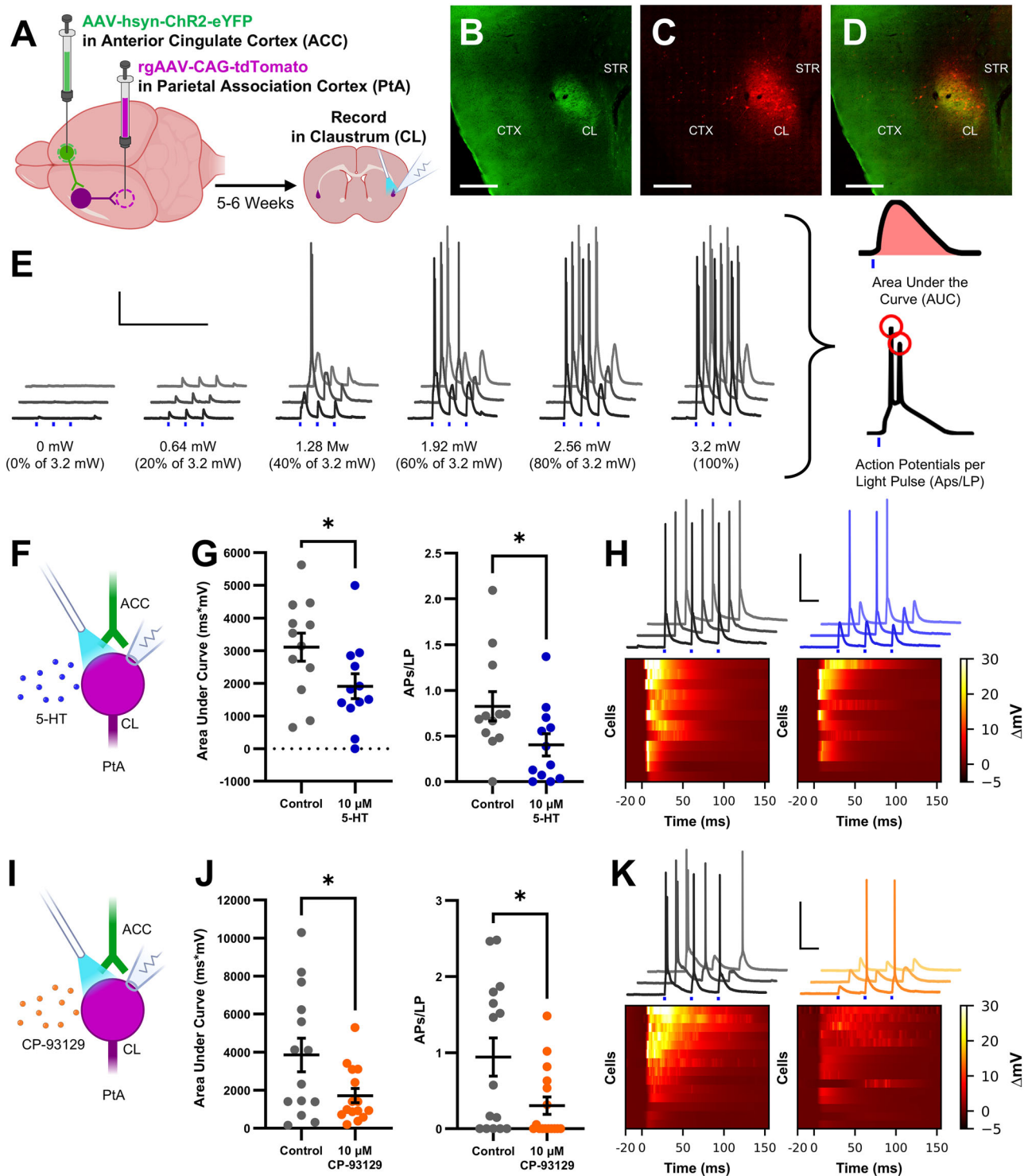
period of 24 h prior to slice recording (3-6 neurons per animal) (Fig. 5I). An elevation of head twitches in the psilocybin recorded animals compared to saline controls (two-tailed Student's t-test, $t_{25} = 13.85$, $p < 0.0001$) (Fig. 5J) confirmed efficacy of the drug. Psilocybin injected animals exhibited lower AUC (two-tailed Student's t-test, $t_{25} = 2.16$, $p = 0.041$) and APs/LP (two-tailed Student's t-test, $t_{25} = 2.32$, $p = 0.029$) compared to saline-injected animals at the 24 h timepoint (Fig. 5K, L). These data suggest that psilocybin induced a lasting depression of the signaling from ACC to PtA-projecting claustrum neurons, via 5-HT$_{1B}$, as psilocin is fully metabolized within 24 h[51–53].

Discussion

Our results show that 5-HT induced a presynaptically-expressed, 5-HT$_{1B}$-mediated synaptic depression of glutamatergic input from the ACC to the claustrum, including PtA-projecting neurons. Additionally, we show that psilocybin recruited 5-HT$_{1B}$ to produce a lasting (up to 24 hr) suppression of ACC input to PtA-projecting claustrum neurons. These findings demonstrate a primary role for 5-HT in regulation of cortico-cortical interactions through the claustrum. Considering the role for the claustrum in supporting cortical networks and the dissolution of these networks in response to psilocybin administration[54],

Fig. 4 | 5-HT or CP-93219 decreased ACC signaling to PtA-projecting claustrum neurons. A Diagram of the dual viral strategy for interrogation of the ACC-claustrum-PtA circuit. **B** Representative image of ACC terminal labeling in claustrum. **C** Representative image of labeling of PtA-projecting neurons in claustrum. **D** Overlay of somata and terminal labeling from **B** and **C**. **E** Experimental diagram corresponding to panels G, H, J, and K. Three light pulses were applied with an inter-pulse interval of 150 ms. This happened every 20 s, for a total of nine stimulations. This was repeated across multiple stimulation intensities. The area under the curve (AUC) and action potentials per light pulse (APs/LP) were determined and averaged across all stimulations. **F** Experimental diagram corresponding to **F** and **G**. **G** Left, the AUC of the voltage response to optical stimulation was lower in neurons recorded after 5-HT (10 μM, 10 min) exposure (n = 12 neurons, from 5 animals) compared to those recorded from the same slices before exposure (n = 12 neurons, from the same 5 animals) (two-tailed Student's t-test, t_{22} = 2.092, p = 0.0482). Right, the average APs/LP was lower after exposure to 5-HT (10 μM, 10 min) compared to those recorded from the same slices before exposure (two-tailed Student's t-test, t_{22} = 2.10, p = 0.048). **H** Top, representative voltage responses to optical

stimulation at baseline (gray) and in 10 μM 5-HT (blue). Bottom, the average voltage response of all neurons recorded, unexposed neurons (left), 5-HT exposed neurons (right). **I** Experimental diagram corresponding to **I** and **J**. **J** Left, the average AUC of the voltage response to optical stimulation was lower in neurons recorded after CP-93129 (10 μM, 10 min) exposure (n = 15, from 4 animals) compared to those recorded from the same slices prior to exposure (n = 14, from the same 4 animals) (two-tailed Student's t-test, t_{27} = 2.30, p = 0.030). Right, the average APs/LP was lower after exposure to CP-93129 (10 μM, 10 min) compared to neurons recorded from the same slices prior to exposure (two-tailed Student's t-test, t_{29} = 2.36, p = 0.025). **K** Top, representative traces of voltage responses to optical stimulation in unexposed (gray) and neurons exposed to 10 μM CP-93129 (orange). Bottom, the average voltage response of all neurons recorded, unexposed neurons (left) and CP-93129 exposed neurons (right). Scale bars are 0.3 mm for **B**–**D**. Scale bars for E are 800 ms (horizontal) by 20 mV (vertical). Scale bars for H and K are 100 ms (horizontal) by 40 mV (vertical). All error bars represent SEM. Source data are provided as a Source Data file.

these results suggest that 5-HT$_{1B}$ may, in part, mediate these and other effects of psilocybin in the brain.

Our findings are in alignment with other observations of 5-HT$_{1B}$-mediated presynaptic depression, which occurs at excitatory corticostriatal synapses in mouse[42,43,45] and in the lateral habenula in rat[44]. Our findings of a 5-HT$_{1B}$-dependent synaptic depression by psilocybin are in accordance with previous findings showing that psilocin, the centrally active metabolite of psilocybin, possesses high affinity for 5-HT$_{1B}$ receptors[55,56]. To our knowledge, this observed synaptic effect represents the first demonstration of a central effect induced by psilocybin that is 5-HT$_{1B}$-dependent; psilocybin is thought to primarily act through 5-HT$_{2A}$, and many acute subjective effects of psychedelics can be attributed to that receptor[57]. However, recent consideration of psychedelic effects has expanded to include other receptors[58] as interest in therapeutic effects of psychedelics that may not require 5-HT$_{2A}$[59], has increased.

The 5-HT$_{1B}$ receptor has been previously shown to produce presynaptic inhibition via inhibition of presynaptic voltage-gated calcium channels[60,61]. This mechanism may explain why miniature release events appeared insensitive to 5-HT or CP-93129, as such release events are independent of voltage-gated calcium channel activity at some synapses[47,62]. Beyond this 5-HT$_{1B}$-mediated effect, other 5-HT-mediated mechanisms modulating claustrum function undoubtedly exist. Mouse and reptile claustrum produce highly synchronous activity during sleep[32,33], which in reptiles is suppressed by a 5-HT$_{1D}$ agonist[33]. Here we observed no effect of a 5-HT$_{1D}$ agonist on the ACC-claustrum synapse, suggesting that any possible 5-HT$_{1D}$ role in the murine claustrum exists outside of the ACC-claustrum synapse. 5-HT$_{2C}$ activation by 5-HT decreases claustrum neuron excitability[63], which while concordant with a general role for 5-HT in suppressing claustrum signaling, is in contrast to the lack of any changes in cellular excitability measures in response to psilocybin injection or 5-HT application to acute brain slices found here. A likely explanation is that these previously reported excitability effects are transient relative to the known persistent effects induced by activation of 5-HT$_{1B}$ and other G$_i$-coupled presynaptic receptors[45,64]. Supporting this notion, we recorded after removal of 5-HT or CP-93129 from the bath solution, and in the case of psilocybin experiments, slices were incubated and recorded in aCSF solution not containing any pharmacological agents.

The dose of psilocybin used here (1 mg/kg) and the dose in humans that produces a decrease in claustrum amplitude of low frequency fluctuation BOLD signal (10 mg/70 kg) can both be considered relatively low for the respective species[34,65,66]. Nevertheless, Barrett, et al.[34] noted significant subjective alterations in conscious experience and here we noted significant head twitch responses at these doses. Barrett et al. (2020) found widespread functional connectivity effects between claustrum and multiple cortical networks and here we found

significant suppression of signaling from ACC to PtA-projecting claustrum neurons. Together this suggests that even relatively low doses of psilocybin alter the activity of the claustrum and its functional relationship with cortex. Since psilocin is a potent agonist of 5-HT$_{2A}$, which is widely expressed across cortex[67,68], and 5-HT$_{1B}$ is additionally expressed in cortex[67,69], 5-HT$_{1B}$-mediated suppression of ACC inputs to cortically-projecting claustrum neurons may be only one component leading to the disruption of cortical networking by psilocybin. As such, we can cautiously conclude that our data provide a potential circuit mechanism for psilocybin-induced alterations in claustrum signaling seen in vivo[34] and lends further support for a claustrum contribution to psychedelic action, as previously proposed[35].

The suppressive effects of 5-HT and psilocybin injection on the ACC-claustrum-PtA circuit cannot be assumed to be universally applied to all cortico-claustro-cortical circuits. Additionally, while pre-administration of a 5-HT$_{1B}$ antagonist before psilocybin suggests the 5-HT$_{1B}$ dependance of ACC-claustrum-PtA circuit suppression by psilocybin, there are no doubt additional effects of psilocybin mediated by other receptors and not captured within this study. Indeed, due to the limitations inherent in pharmacological manipulations in acute brain slices used herein, the role of other receptors cannot be ruled out. Many other 5-HT receptors are expressed within the claustrum such as 5-HT$_{2A}$, 5-HT$_{2C}$, and 5-HT$_{1A}$[23,25,26,70–75]. Some effects within cortico-claustro-cortical circuits may additionally occur at the claustrum-cortex synapse, which was not assayed within this study. Additionally, some effects of psilocybin in other regions, such as increases in spine density in cortex, do not fully appear until more than a day after drug administration[76].

In conclusion, input from the ACC to the claustrum is required for optimal performance under cognitive demand[40] and the claustrum itself is implicated in instantiation of cortical networks[16,19]. Considering the present report that 5-HT depresses glutamate release from ACC inputs to the claustrum, it is possible that this effect may serve as a gain-control mechanism for claustrum control of downstream cortices. Alternatively, if this effect is differentially expressed across various cortical inputs to the claustrum, 5-HT may serve to bias claustrum signaling toward specific circuits over others. Thus, 5-HT signaling is poised to modulate cortico-claustral transmission in concert with acetylcholine, which is co-released with GABA to induce 'toggling' of efficient information flow to either subcortical or cortical claustrum projection targets[77]. Considering that exogenous drugs, such as psilocybin demonstrated herein, may ultimately activate 5-HT$_{1B}$ receptors to significantly modulate cortico-claustro-cortical signaling, this may contribute to the cognitive or subjective effects of psilocybin and other 5-HT$_{1B}$ agonists. Further investigation is required to fully understand when this 5-HT$_{1B}$ mechanism is engaged in vivo and how it may contribute to the potential therapeutic effects of psilocybin.
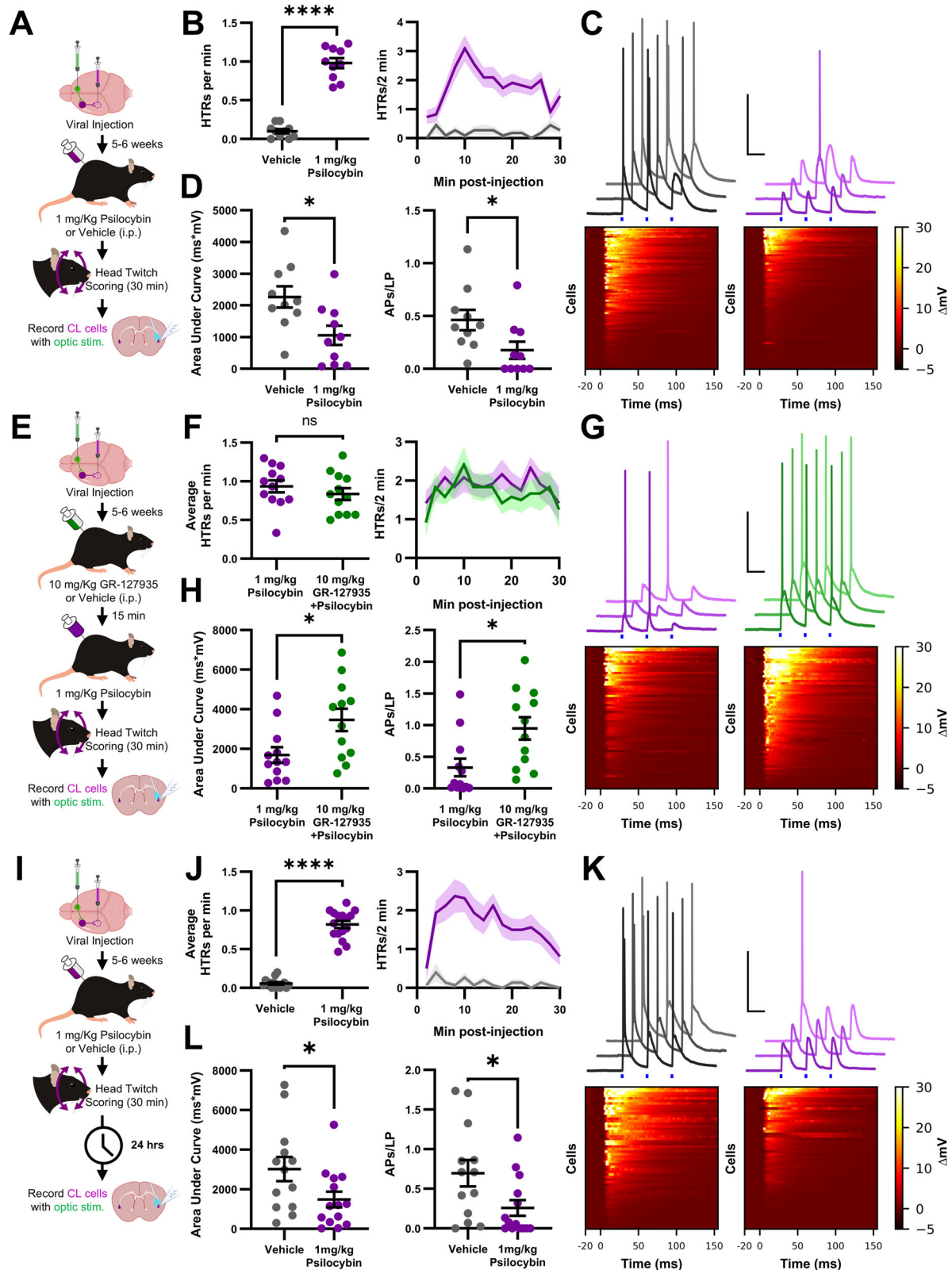
Methods

Animals

117 C57BL/6 (wild type) male and female mice were used for slice electrophysiology experiments. All cohorts, unless otherwise stated, contained equal numbers of male and female mice. Mice were 10–20 weeks of age at the time of experimentation and group-housed with food and water available *ad libitum*. All mice were on a 12 h light/dark cycle beginning at 7:00 a.m. and all behavioral experiments were performed during the light cycle. For experiments with comparisons across animals, control and experimental groups were drawn from the same litters to minimize potential litter effects. Four mice were used for histology and verification of surgical coordinates. Animals were euthanized by inhalation of an overdose of isoflurane, followed by decapitation, in accordance with University of

Fig. 5 | Psilocybin injection suppressed ACC activation of PtA-projecting claustrum neurons in a 5-HT$_{1B}$-dependent manner. A Experimental timeline, corresponding to **B–D**. **B** Left, average rate of head twitches in animals injected with 1 mg/kg psilocybin (N = 10) was significantly elevated over vehicle injected animals (N = 10) (two-tailed Student's t-test, t_{18} = 12.45, p = 3 × 10^{-10}). Right, average head twitches over the 30-minute scoring period immediately post psilocybin injection. **C** Top, representative voltage responses in neurons from vehicle-injected (gray) or psilocybin-injected (purple) animals. Bottom, the average voltage response of all neurons recorded (4–10 neurons per animal): neurons from vehicle-injected animals (left), neurons from psilocybin injected animals (right). **D** Average AUC (left) and APs/LP (right) across all neurons recorded. Both AUC (two-tailed Student's t-test, t_{18} = 2.67, p = 0.016) and APs/LP (two-tailed Student's t-test, t_{18} = 2.26, p = 0.036) were lower in the psilocybin-injected animals. **E** Experimental diagram corresponding to **F–G**. **F** Left, average rate of head twitches was not different between animals pre-injected with the 5-HT$_{1B/D}$ antagonist 10 mg/kg GR-127935 (N = 12) or vehicle (N = 12) (t_{22} = 0.91, p = 0.37, two-tailed Student's t-test). Right, average head twitches immediately post psilocybin injection with (green) or without (purple) GR-127935 pre-injection. **G** Top, representative voltage responses in neurons from vehicle pre-injected animals (purple) and animals pre-injected with GR-127935 (green). Bottom, the average voltage response of all neurons recorded (4-7 neurons per animal): vehicle (left) and psilocybin with GR-127935 pre-injection (right). **H** Animals pre-injected with GR-127935 exhibited higher average AUC (t_{22} = 2.55, p=0.018, two-tailed Student's t-test) and APs/LP (t_{22} = 2.73, p = 0.012, two-tailed Student's t-test) than vehicle pre-injected animals. **I** Diagram of the experimental timeline, corresponding to **J–L. J** Left, average rate of head twitches in animals injected with 1 mg/kg psilocybin (N = 13) was significantly elevated over vehicle injected animals (N = 14) (t_{25} = 13.85, p = 3 × 10^{-13}, two-tailed Student's t-test). Right, average head twitches immediately post psilocybin injection. **K** Top, representative voltage responses in neurons from vehicle-injected (gray) or psilocybin-injected (purple) animals, recorded 24 h after drug injection. Bottom, the average voltage response of all neurons (3-6 neurons per animal): vehicle-injected (left), psilocybin-injected (right). **L** Animals injected with psilocybin showed lower AUC (t_{25} = 2.16, p = 0.041, two-tailed Student's t-test) and APs/LP (t_{25} = 2.32, p = 0.029, two-tailed Student's t-test) 24 h after drug injection compared to vehicle-injected animals. Scale bars in **C**, **G**, and **K** are 100 ms (horizontal) by 40 mV (vertical). All error bars represent SEM. Source data are provided as a Source Data file.

Maryland IACUC guidelines. This study was performed in accordance with the National Institutes of Health Guide for Care and Use of Laboratory Animals and the University of Maryland, School of Medicine, Animal Care and Use Committee (approval no. 0522009).

Viral Vectors and Stereotaxic Procedures

Mice were anesthetized via inhalation of isoflurane (3.5%) prior to being placed in a mouse stereotaxic frame (David KOPF instruments, Tujunga CA). Anesthesia was subsequently maintained with inhaled isoflurane (1%). Following incision of the scalp, small holes were drilled in the surface of the skull using a drill with a 0.5 nm diameter ball mill carbide drill bit. 250 nL of an adeno-associated virus (AAV) vector expressing Chr2 (AAV5-hSyn-ChR2(H134R)-EYFP; Addgene: 26973-AAV5) was injected into ACC. The coordinates utilized for ACC were anterior-posterior: +1.00 mm, medial-lateral: ±0.30 mm, dorsal-ventral: −1.10 mm. For experiments specifically targeting the ACC input to PtA-projecting claustrum neurons, mice received an additional injection 150 nl of a retrograde AAV expressing tdTomato (rgAAV-CAG-tdTomato; Addgene: 59462-AAVrg) into PtA. The coordinates utilized for PtA were anterior-posterior: −1.90 mm, medial-lateral: ±1.40 mm, dorsal-ventral: -0.40 mm. All injection sites were checked for accuracy prior to experimentation. For all coordinates, anterior-posterior and medio-lateral coordinates were measured from bregma and dorsal-ventral coordinates were measured from top of brain surface.

Brain slice preparation

Male and female wildtype C57BL/6 mice between the ages of 10-16 weeks were anesthetized with isoflurane prior to decapitation. The brain was immediately removed and placed within an ice chilled cutting solution composed of 194 mM Sucrose, 30 mM NaCl, 4.5 mM KCl, 1 mM MgCl$_2$, 26 mM NaHCO$_3$, 1.2 mM NaH$_2$PO$_4$, 10 mM Glucose. 250 μm thick coronal slices were then cut with a Leica VT1200 vibrating microtome. The vibratome chamber was ice-chilled prior to cutting and was filled with oxygenated cutting solution. Slices were incubated at 32 °C in oxygenated artificial cerebrospinal fluid (aCSF). The aCSF (adjusted to 308-315 mOsm with sucrose) contained 124 mM NaCl, 4.5 mM KCl, 1 mM MgCl$_2$, 26 mM NaHCO$_3$, 1.2 mM NaH$_2$PO$_4$, 10 mM Glucose, and 2 mM CaCl$_2$. The cutting solution and aCSF were prepared with deionized water (18.2 MΩ-cm), filtered (0.22 μm), and bubbled with 95% O$_2$ and 5% CO$_2$ for at least 15 min prior to use and throughout slice preparation and recording. After incubation, slices were maintained at room temperature until whole-cell patch-clamp recording, which was performed in the same aCSF formulation used for incubation. For experiments recording asynchronous release events, an alternative aCSF formulation was used for recording only, in which 2 mM CaCl$_2$ was replaced with 2 mM SrCl$_2$.

Whole-cell patch-clamp electrophysiological recordings

Whole-cell recordings were performed at 28–30 °C using borosilicate glass recording pipettes of 2.5–4.5MΩ resistance. For recordings performed in current clamp configuration, recording pipettes were filled with a potassium-based solution (300–308 mOsm; pH 7.3) composed of 126 mM potassium gluconate, 4 mM KCL, 10 mM HEPES, 4 mM Mg-ATP, 0.3 mM Na-GTP and 10 mM phosphocreatine. For recordings performed in voltage clamp configuration, recording pipettes were filled with a CsMeSO$_3$-based solution (300–308 mOsm; pH 7.3) composed of 120 mM CsMeSO$_3$, 5 mM NaCl, 10 mM TEA-Cl, 10 mM HEPES, 1.1 mM EGTA, 0.3 mM Na-GTP, and 4 mM Mg-ATP. Clampex software (Version 10.4; Molecular Devices) was used for all electrophysiological recordings. During all voltage clamp recordings, neurons were held at −60 mV for the duration of the recording. Recordings were filtered at 2 kHz and digitized at 10 kHz using MultiClamp 700B software (Molecular Devices). In experiments utilizing ChR2 stimulation, 5 ms light pulses (470 nm wavelength) were delivered to the slice via an optical fiber to evoke presynaptic transmitter release. In experiments selectively targeting ACC input to PtA-projecting claustrum neurons, recordings were derived only from fluorescent retrogradely-labeled claustrum projection neurons. In all experiments, expression of eYFP in ACC terminals was utilized to identify the claustrum within the slice.

Drugs

Bath applied drugs used in electrophysiological experiments (TTX, PTX, 4-AP, CP-93129, SB-216641, 5-HT, PNU-142633, GR-127935, LY-310762) were obtained from Tocris Bioscience. Injected drugs, Psilocybin (Cayman Chemical) and GR-127935 (Tocris Bioscience) were dissolved in 0.9% Sodium Chloride (USP) at 0.1 mg/ml and 2 mg/ml respectively and stored at −20 °C until use and were injected intraperitoneally (i.p).

Head twitch responses

A head twitch response is a rapid head movement that occurs in mice after administration of psychedelic drugs, mediated by 5-HT$_{2A}$[48–50]. Recording of these events was used to confirm the activity of psilocybin. Immediately after psilocybin injection, animals were placed in a 19.5 cm diameter, 25 cm tall cylindrical chamber for video recording of head twitch responses. Head twitches were semi-automatically scored using a human supervised combination of machine-learning based pose estimation via SLEAP v1.3.3[78] and custom python code. Automated continuous tracking of the ears allowed identification of candidate head twitches as instances of ear acceleration exceeding an empirically determined threshold value. Candidate events were then extracted from video and visually confirmed by a trained human experimenter.

Histology

Mice were perfused with room temperature 0.1 M phosphate-buffered saline (PBS), pH 7.3, and then with chilled (4 °C) paraformaldehyde (PFA) solution in PBS. After extraction, brains were post-fixed in 4% PFA solution overnight. Brains were then sliced to 50 μm thickness using an Integraslice 7550 MM vibrating microtome (Campden Instruments, Loughborough, England). Slices were then mounted using ProLong Gold antifade reagent (Invitrogen) and imaged using a CSU-W1 confocal microscope or fluorescence microscope (Nikon, Minato, Tokyo, Japan).

Data analysis and statistics

Whole-cell patch-clamp electrophysiology data were analyzed using Minhee Analysis Package[79], Python, and pyabf v2.3.8[80], with subsequent statistical analysis performed in Prism v10.3.1 (GraphPad Software; La Jolla, CA). Significance levels are denoted as *$P < 0.05$, **$P < 0.01$, ***$P < 0.001$, ****$P < 0.0001$; ns, not significant for all figures.

Reporting summary

Further information on research design is available in the Nature Portfolio Reporting Summary linked to this article.

Data availability

None. Source data are provided with this paper.

Code availability

The python code used in this study is available at https://github.com/MathurLabUMSOM/maddenetal2025.

References

1. McCormick, D. A., Nestvogel, D. B. & He, B. J. Neuromodulation of brain state and behavior. *Annu. Rev. Neurosci.* **43**, 391–415 (2020).
2. Lee, S.-H. & Dan, Y. Neuromodulation of brain states. *Neuron* **76**, 209–222 (2012).
3. Cohen, J. Y., Haesler, S., Vong, L., Lowell, B. B. & Uchida, N. Neuron-type-specific signals for reward and punishment in the ventral tegmental area. *Nature* **482**, 85–88 (2012).
4. Bromberg-Martin, E. S., Hikosaka, O. & Nakamura, K. Coding of task reward value in the dorsal raphe nucleus. *J. Neurosci.* **30**, 6262–6272 (2010).
5. Luo, M., Zhou, J. & Liu, Z. Reward processing by the dorsal raphe nucleus: 5-HT and beyond. *Learn. Mem.* **22**, 452–460 (2015).
6. Nakamura, K. The role of the dorsal raphé nucleus in reward-seeking behavior. *Front. Integr. Neurosci.* **7**, 60 (2013).
7. Nakamura, K., Matsumoto, M. & Hikosaka, O. Reward-dependent modulation of neuronal activity in the primate dorsal raphe nucleus. *J. Neurosci.* **28**, 5331–5343 (2008).
8. Grossman, C. D., Bari, B. A. & Cohen, J. Y. Serotonin neurons modulate learning rate through uncertainty. *Curr. Biol.* **32**, 586–599. e587 (2022).
9. Gonzalez-Burgos, G., Kroener, S., Seamans, J. K., Lewis, D. A. & Barrionuevo, G. Dopaminergic modulation of short-term synaptic plasticity in fast-spiking interneurons of primate dorsolateral prefrontal cortex. *J. Neurophysiol.* **94**, 4168–4177 (2005).
10. Pafundo, D. E., Miyamae, T., Lewis, D. A. & Gonzalez-Burgos, G. Cholinergic modulation of neuronal excitability and recurrent excitation-inhibition in prefrontal cortex circuits: implications for gamma oscillations. *J. Physiol.* **591**, 4725–4748 (2013).
11. Su, Z. & Cohen, J. Y. Two types of locus coeruleus norepinephrine neurons drive reinforcement learning. *BioRxiv,* 2022.2012.2008.519670 (2022).
12. Ogawa, S. K., Cohen, J. Y., Hwang, D., Uchida, N. & Watabe-Uchida, M. Organization of monosynaptic inputs to the serotonin and dopamine neuromodulatory systems. *Cell Rep.* **8**, 1105–1118 (2014).
13. Williams, G. V. & Goldman-Rakic, P. S. Modulation of memory fields by dopamine Dl receptors in prefrontal cortex. *Nature* **376**, 572–575 (1995).
14. Mrzijak, L., Pappy, M., Leranth, C. & Goldman-Rakic, P. S. Cholinergic synaptic circuitry in the macaque prefrontal cortex. *J. Comp. Neurol.* **357**, 603–617 (1995).
15. Gao, W.-J., Wang, Y. & Goldman-Rakic, P. S. Dopamine modulation of perisomatic and peridendritic inhibition in prefrontal cortex. *J. Neurosci.* **23**, 1622–1630 (2003).
16. Madden, M. B. et al. A role for the claustrum in cognitive control. *Trends Cogn. Sci.* **26**, 1133–1152 (2022).
17. Krimmel, S. R. et al. Resting state functional connectivity and cognitive task-related activation of the human claustrum. *Neuroimage* **196**, 59–67 (2019).
18. White, M. G. et al. The mouse claustrum is required for optimal behavioral performance under high cognitive demand. *Biol. Psychiatry* **88**, 719–726 (2020).
19. Stewart, B. W. et al. Pathological claustrum activity drives aberrant cognitive network processing in human chronic pain. *Curr. Biol.* **34**, 1953–1966. e1956 (2024).
20. Qadir, H. et al. The mouse claustrum synaptically connects cortical network motifs. *Cell Rep.* **41**, 111860 (2022).
21. Chia, Z., Augustine, G. J. & Silberberg, G. Synaptic connectivity between the cortex and claustrum is organized into functional modules. *Curr. Biol.* **30**, 2777–2790 (2020).
22. White, M. G. & Mathur, B. N. Claustrum circuit components for top-down input processing and cortical broadcast. *Brain Struct. Funct.* **223**, 3945–3958 (2018).
23. Rioux, A. et al. Adaptive changes of serotonin 5-HT2A receptors in mice lacking the serotonin transporter. *Neurosci. Lett.* **262**, 113–116 (1999).
24. Mengod, G. et al. 5-HT receptors in mammalian brain: receptor autoradiography and in situ hybridization studies of new ligands and newly identified receptors. *Histochem. J.* **28**, 747–758 (1996).
25. Pompeiano, M., Palacios, J. M. & Mengod, G. Distribution of the serotonin 5-HT2 receptor family mRNAs: comparison between 5-HT2A and 5-HT2C receptors. *Mol. Brain Res.* **23**, 163–178 (1994).
26. Hamada, S. et al. Localization of 5-HT2A receptor in rat cerebral cortex and olfactory system revealed by immunohistochemistry using two antibodies raised in rabbit and chicken. *Mol. Brain Res.* **54**, 199–211 (1998).
27. Hall, H., Farde, L., Halldin, C., Lundkvist, C. & Sedvall, G. Autoradiographic localization of 5-HT2A receptors in the human brain using [3H] M100907 and [11C] M100907. *Synapse* **38**, 421–431 (2000).
28. Bruinvels, A. T., Landwehrmeyer, B., Probst, A., Palacios, J. M. & Hoyer, D. A comparative autoradiographic study of 5-HT1D binding sites in human and guinea-pig brain using different radioligands. *Mol. Brain Res.* **21**, 19–29 (1994).
29. Pasqualetti, M., Nardi, I., Ladinsky, H., Marazziti, D. & Cassano, G. B. Comparative anatomical distribution of serotonin 1A, 1Dα and 2A receptor mRNAs in human brain postmorten. *Mol. Brain Res.* **39**, 223–233 (1996).
30. Zingg, B., Dong, H. W., Tao, H. W. & Zhang, L. I. Input-output organization of the mouse claustrum. *J. Comp. Neurol.* **526**, 2428–2443 (2018).
31. Kato, T. et al. Oscillatory population-level activity of dorsal raphe serotonergic neurons is inscribed in sleep structure. *J. Neurosci.* **42**, 7244–7255 (2022).
32. Narikiyo, K. et al. The claustrum coordinates cortical slow-wave activity. *Nat. Neurosci.* **23**, 741–753 (2020).
33. Norimoto, H. et al. A claustrum in reptiles and its role in slow-wave sleep. *Nature* **578**, 413–418 (2020).

34. Barrett, F. S., Krimmel, S. R., Griffiths, R. R., Seminowicz, D. A. & Mathur, B. N. Psilocybin acutely alters the functional connectivity of the claustrum with brain networks that support perception, memory, and attention. *NeuroImage* **218**, 116980 (2020).

35. Doss, M. K. et al. Models of psychedelic drug action: modulation of cortical-subcortical circuits. *Brain* **145**, 441 (2021).

36. Nichols, D. E. Psychedelics. *Pharmacol. Rev.* **68**, 264–355 (2016).

37. Stiefel, K. M., Merrifield, A. & Holcombe, A. O. The claustrum's proposed role in consciousness is supported by the effect and target localization of Salvia divinorum. *Front. Integr. Neurosci.* **8**, 20 (2014).

38. White, M. G. et al. Cortical hierarchy governs rat claustrocortical circuit organization. *J. Comp. Neurol.* **525**, 1347–1362 (2017).

39. Atlan, G., Terem, A., Peretz-Rivlin, N., Groysman, M. & Citri, A. Mapping synaptic cortico-claustral connectivity in the mouse. *J. Comp. Neurol.* **525**, 1381–1402 (2017).

40. White, M. G. et al. Anterior cingulate cortex input to the claustrum is required for top-down action control. *Cell Rep.* **22**, 84–95 (2018).

41. Mathur, B. N. & Lovinger, D. M. Serotonergic action on dorsal striatal function. *Parkinsonism Relat. Disord.* **18**, S129–S131 (2012).

42. Dölen, G., Darvishzadeh, A., Huang, K. W. & Malenka, R. C. Social reward requires coordinated activity of nucleus accumbens oxytocin and serotonin. *Nature* **501**, 179–184 (2013).

43. Christoffel, D. J. et al. Selective filtering of excitatory inputs to nucleus accumbens by dopamine and serotonin. *Proc. Natl. Acad. Sci. USA* **118**, e2106648118 (2021).

44. Hwang, E.-K. & Chung, J. -m. 5HT1B receptor-mediated pre-synaptic depression of excitatory inputs to the rat lateral habenula. *Neuropharmacology* **81**, 153–165 (2014).

45. Mathur, B. N., Capik, N. A., Alvarez, V. A. & Lovinger, D. M. Serotonin induces long-term depression at corticostriatal synapses. *J. Neurosci.* **31**, 7402–7411 (2011).

46. Bonaventure, P. et al. Detailed mapping of serotonin 5-HT1B and 5-HT1D receptor messenger RNA and ligand binding sites in guinea-pig brain and trigeminal ganglion: clues for function. *Neuroscience* **82**, 469–484 (1997).

47. Kaeser, P. S. & Regehr, W. G. Molecular mechanisms for synchronous, asynchronous, and spontaneous neurotransmitter release. *Annu. Rev. Physiol.* **76**, 333–363 (2014).

48. Halberstadt, A. L. & Geyer, M. A. Multiple receptors contribute to the behavioral effects of indoleamine hallucinogens. *Neuropharmacology* **61**, 364–381 (2011).

49. Halberstadt, A. L. & Geyer, M. A. Characterization of the head-twitch response induced by hallucinogens in mice: detection of the behavior based on the dynamics of head movement. *Psychopharmacology* **227**, 727–739 (2013).

50. Canal, C. E. & Morgan, D. Head-twitch response in rodents induced by the hallucinogen 2, 5-dimethoxy-4-iodoamphetamine: a comprehensive history, a re-evaluation of mechanisms, and its utility as a model. *Drug Test. Anal.* **4**, 556–576 (2012).

51. Holze, F., Becker, A. M., Kolaczynska, K. E., Duthaler, U. & Liechti, M. E. Pharmacokinetics and pharmacodynamics of oral psilocybin administration in healthy participants. *Clin. Pharmacol. Ther.* **113**, 822–831 (2023).

52. Thomann, J. et al. In vitro and in vivo metabolism of psilocybin's active metabolite psilocin. *Front Pharm.* **15**, 1391689 (2024).

53. Khajavinia, A. et al. Addressing a major interference in the quantification of psilocin in mouse plasma: Development of a validated liquid chromatography tandem mass spectrometry method. *J. Chromatogr. A* **1730**, 465123 (2024).

54. Siegel, J. S. et al. Psilocybin desynchronizes the human brain. *Nature* **632**, 131–138 (2024).

55. Roth, B. & Driscol, J. PDSP Ki database. *Psychoactive Drug Screening Program (PDSP); United States National Institute of Mental Health, University of North Carolina: Chapel Hill, NC, USA* (2011).

56. Roth, B. L., Lopez, E., Patel, S. & Kroeze, W. K. The multiplicity of serotonin receptors: uselessly diverse molecules or an embarrassment of riches?. *Neuroscientist* **6**, 252–262 (2000).

57. Halberstadt, A. L. Recent advances in the neuropsychopharmacology of serotonergic hallucinogens. *Behav. Brain Res.* **277**, 99–120 (2015).

58. Cameron, L. P. et al. Beyond the 5-HT2A receptor: classic and nonclassic targets in psychedelic drug action. *J. Neurosci.* **43**, 7472–7482 (2023).

59. Hesselgrave, N., Troppoli, T. A., Wulff, A. B., Cole, A. B. & Thompson, S. M. Harnessing psilocybin: antidepressant-like behavioral and synaptic actions of psilocybin are independent of 5-HT2R activation in mice. *Proc. Natl. Acad. Sci. USA* **118**, e2022489118 (2021).

60. Choi, I. S. et al. 5-HT1B receptors inhibit glutamate release from primary afferent terminals in rat medullary dorsal horn neurons. *Br. J. Pharmacol.* **167**, 356–367 (2012).

61. Mizutani, H., Hori, T. & Takahashi, T. 5-HT1B receptor-mediated presynaptic inhibition at the calyx of Held of immature rats. *Eur. J. Neurosci.* **24**, 1946–1954 (2006).

62. Lee, B. J. et al. Voltage-gated calcium channels contribute to spontaneous glutamate release directly via nanodomain coupling or indirectly via calmodulin. *Prog. Neurobiol.* **208**, 102182 (2022).

63. Anderson, T. L. et al. Distinct 5-HT receptor subtypes regulate claustrum excitability by serotonin and the psychedelic, DOI. *Prog. Neurobiol.* **240**, 102660 (2024).

64. Atwood, B. K., Lovinger, D. M. & Mathur, B. N. Presynaptic long-term depression mediated by Gi/o-coupled receptors. *Trends Neurosci.* **37**, 663–673 (2014).

65. Carbonaro, T. M., Johnson, M. W., Hurwitz, E. & Griffiths, R. R. Double-blind comparison of the two hallucinogens psilocybin and dextromethorphan: similarities and differences in subjective experiences. *Psychopharmacology* **235**, 521–534 (2018).

66. Schindler, E. A. et al. Psilocybin pulse regimen reduces cluster headache attack frequency in the blinded extension phase of a randomized controlled trial. *J. Neurol. Sci.* **460**, 122993 (2024).

67. Beliveau, V. et al. A high-resolution in vivo atlas of the human brain's serotonin system. *J. Neurosci.* **37**, 120–128 (2017).

68. Weber, E. T. & Andrade, R. Htr2a gene and 5-HT2A receptor expression in the cerebral cortex studied using genetically modified mice. *Front. Neurosci.* **4**, 36 (2010).

69. Bruinvels, A. T. et al. Localization of 5-HT1B, 5-HT1Dα, 5-HT1E and 5-HT1F receptor messenger RNA in rodent and primate brain. *Neuropharmacology* **33**, 367–386 (1994).

70. Mengod, G., Pompeiano, M. & Marti, M. I. Localization of the mRNA for the 5-HT2 receptor by in situ hybridization histochemistry. Correlation with the distribution of receptor sites. *Brain Res.* **524**, 139–143 (1990).

71. Pazos, A., Probst, A. & Palacios, J. Serotonin receptors in the human brain—III. Autoradiographic mapping of serotonin-1 receptors. *Neuroscience* **21**, 97–122 (1987).

72. Wright, D., Seroogy, K., Lundgren, K., Davis, B. & Jennes, L. Comparative localization of serotonin1A, 1C, and 2 receptor subtype mRNAs in rat brain. *J. Comp. Neurol.* **351**, 357–373 (1995).

73. Gawlinski, D. et al. Adaptive mechanisms following antidepressant drugs: Focus on serotonin 5-HT2A receptors. *Pharm. Rep.* **71**, 994–1000 (2019).

74. Kinsey, A. M., Wainwright, A., Heavens, R., Sirinathsinghji, D. J. & Oliver, K. R. Distribution of 5-HT5A, 5-HT5B, 5-HT6 and 5-HT7 receptor mRNAs in the rat brain. *Mol. Brain Res.* **88**, 194–198 (2001).

75. Ward, R. P. & Dorsa, D. M. Colocalization of serotonin receptor subtypes 5-HT2A, 5-HT2C, and 5-HT6 with neuropeptides in rat striatum. *J. Comp. Neurol.* **370**, 405–414 (1996).

76. Shao, L.-X. et al. Psilocybin induces rapid and persistent growth of dendritic spines in frontal cortex in vivo. *Neuron* **109**, 2535–2544.e2534 (2021).

77. Nair, A., Teo, Y. Y., Augustine, G. J. & Graf, M. A functional logic for neurotransmitter corelease in the cholinergic forebrain pathway. *Proc. Natl. Acad. Sci. USA* **120**, e2218830120 (2023).

78. Pereira, T. D. et al. SLEAP: A deep learning system for multi-animal pose tracking. *Nat. Methods* **19**, 486–495 (2022).

79. Kim, Y. G., Shin, J. J. & Kim, S. J. Minhee Analysis Package: an integrated software package for detection and management of spontaneous synaptic events. *Mol. Brain* **14**, 1–17 (2021).

80. Harden, S. W. pyABF 2.3.8. [Online]. Available: (https://pypi.org/project/pyabf) (2022).

Acknowledgements

Author contributions

Conceptualization M.B.M., B.N.M.; Surgical Procedure M.B.M., S.H.S.; Electrophysiology M.B.M., C.S.; Behavioral Scoring, M.B.M., B.V., J.K., K.S.D.P., S.B.E.W.; Imaging M.B.M., S.H.S., K.S.D.P.; Data Analysis M.B.M.; Writing (Original Draft) M.B.M., B.N.M.; Review & Editing M.B.M., C.S., B.V., J.K., K.S.D.P., S.H.S., A.C.P., S.B.E.W., B.N.M.; Supervision A.C.P., S.B.E.W., B.N.M.; Project Administration B.N.M.; Funding Acquisition M.B.M., S.B.E.W., B.N.M.

Competing interests

The authors declare no competing interests.

Additional information